

# ENCODER-MINIMAL AND DECODER-MINIMAL FRAMEWORK FOR REMOTE SENSING IMAGE DEHAZING

Yuanbo Wen<sup>1</sup> Tao Gao<sup>1\*</sup> Ziqi Li<sup>1</sup> Jing Zhang<sup>2</sup> Ting Chen<sup>1\*</sup>

<sup>1</sup> School of Information Engineering, Chang'an University, Xi'an, China; <sup>2</sup> College of Engineering and Computer Science, Australian National University, Canberra, ACT, Australia

## ABSTRACT

Haze obscures remote sensing images, hindering valuable information extraction. To this end, we propose RSHazeNet, an encoder-minimal and decoder-minimal framework for efficient remote sensing image dehazing. Specifically, regarding the process of merging features within the same level, we develop an innovative module called intra-level transposed fusion module (ITFM). This module employs adaptive transposed self-attention to capture comprehensive context-aware information, facilitating the robust context-aware feature fusion. Meanwhile, we present a cross-level multi-view interaction module (CMIM) to enable effective interactions between features from various levels, mitigating the loss of information due to the repeated sampling operations. In addition, we propose a multi-view progressive extraction block (MPEB) that partitions the features into four distinct components and employs convolution with varying kernel sizes, groups, and dilation factors to facilitate view-progressive feature learning. Extensive experiments demonstrate the superiority of our proposed RSHazeNet. We release the source code and all pre-trained models at <https://github.com/chdwyb/RSHazeNet>.

**Index Terms**— Image dehazing, remote sensing image, computer vision, efficient network

## 1. INTRODUCTION

Haze emerges as a prevalent meteorological phenomenon significantly compromising remote sensing image quality. It leads to a reduction in image contrast and color fidelity, subsequently impeding various observation applications such as image classification [1], modality translation [2], and image super-resolution [3]. Consequently, remote sensing image dehazing holds practical significance in enhancing the quality of captured images affected by haze conditions.

<sup>1</sup>Corresponding author: Tao Gao, Ting Chen

<sup>2</sup>This research was partially supported by the National Key R & D Program of China under Grants 2019YFE0108300, the National Natural Science Foundation of China under Grants 52172379, 62001058 and U1864204, the Fundamental Research Funds for the Central University under Grants 300102242901.

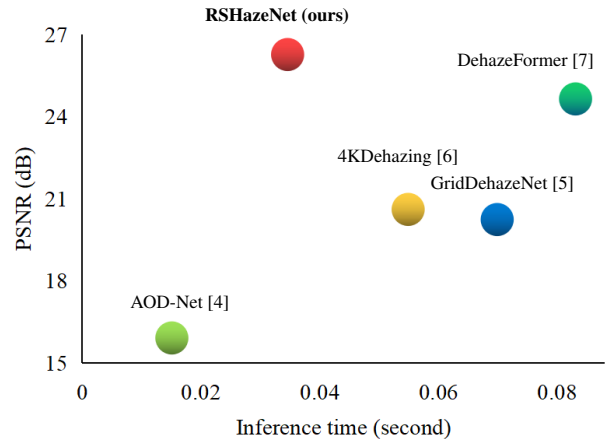


**Fig. 1.** Comparative analysis of efficiency in remote sensing image dehazing approaches. Our novel approach, RSHazeNet, exhibits superior performance in terms of both metrical scores and computational efficiency.

Remote sensing image is always in large resolution while the intensity and distribution of haze are more various. Therefore, most existing dehazing methods [4, 7–11] may not be well-suited for remote sensing image dehazing. In response, DADN [12] introduces a prior-based dense attentive network that leverages dense blocks and attention blocks. FCTF-Net [13] adopts a two-stage framework, while DCRD-Net [14] employs a dual-step cascaded residual dense network to directly reconstruct the background. Additionally, H2RL-Net [15] proposes a multi-scale architecture to mitigate haze degradation. M2SCN [9] incorporates a multi-model joint estimation module and a self-correcting module to construct an end-to-end network. More recently, DehazeFormer [7] introduces a modified normalization layer and a spatial information aggregation scheme. However, these methods face challenges in striking the optimal balance between image quality and inference time.

In this work, we redirect our attention towards skip connections and propose an encoder-minimal and decoder-minimal approach. As depicted in Figure 2, the encoding and decoding stages solely consist of down-sampling and up-sampling operations. Within u-shaped structures, we in-

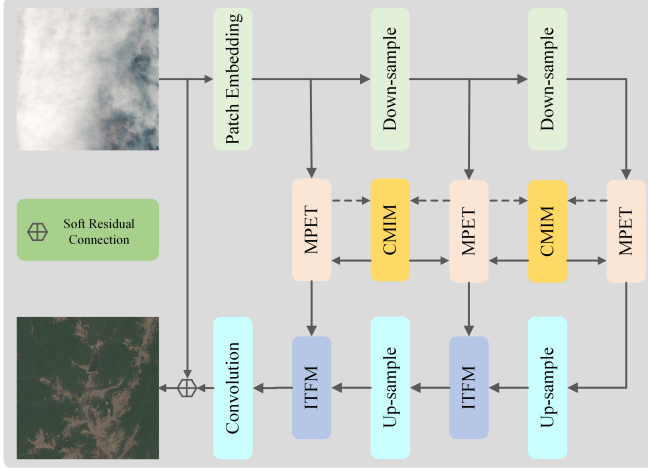


**Fig. 2.** Architectural overview of our proposed encoder-minimal and decoder-minimal RSHazeNet for remote sensing image dehazing.

roduce a intra-level transposed fusion module (ITFM), which incorporates adaptive pooling to capture global spatial information and leverages efficient transposed self-attention to compute attention maps, amalgamating information from distinct feature planes and extracting context-wise attention. By adopting ITFM, we significantly mitigate the computational complexity associated with self-attention and effectively harness global enhanced information to fuse features.

Existing methods exhibit a lack of capability to establish interactions across different levels, resulting in the hindered flow of information between multi-scale features. To this end, we present a novel module called cross-level multi-scale interaction module (CMIM), which facilitates feature interaction between two features of varying resolutions. In CMIM, we employ transposed self-attention to compute attention maps [16]. Specifically, the query representation  $Q$  and key representation  $K$  are derived from the input features at level  $l$  and level  $l - 1$ , respectively. We generate two value representations, which are both enhanced by the same interacting attention map, thus enabling features to flow at different stages and avoid the information loss due to the repeated sampling operations.

Moreover, we introduce a multi-view progressive extraction block (MPEB). Unlike employing  $3 \times 3$  convolutions [17], MPEB exclusively utilizes channel-wise interactions accomplished through  $1 \times 1$  convolutions. To capture the multi-view features from the remaining three quarters of the input, we incorporate grouped convolutions with distinct receptive fields and dilation factors. By adopting MPEB, we not only achieve channel-wise information interaction, but also extract multi-view spatial-wise features. This allows the network to capture different viewpoints of the input features, providing a more robust and discriminative representation.

The overall architecture of our proposed RSHazeNet is

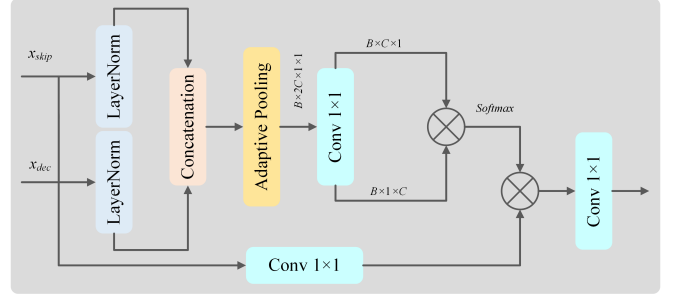


**Fig. 3.** Illustration of our proposed intra-level transposed fusion module (ITFM). It utilizes the adaptive spatial features to calculate the channel-wise attention map and further conduct context-based fusion.

depicted in Figure 2, which achieves the best trade-off between image quality and inference time. We summarize our contributions as follows: 1) We devise a novel architectural design strategy that shifts the emphasis onto skip connections instead of encoders and decoders. 2) An intra-level transposed fusion module that incorporates global information to facilitate the comprehensive and context-aware fusion process. 3) A cross-level multi-scale interaction module that enables effective communication and collaboration between different levels, ensuring that valuable information is preserved and shared. 4) We present a multi-view progressive extraction block that accomplishes both channel-wise interaction and spatial-wise multi-view feature extraction.

## 2. PROPOSED METHOD

### 2.1. Intra-level Transposed Fusion Module

To overcome the limitations in effectively aggregating information from different feature planes, we propose an intra-level transposed fusion module (ITFM) as illustrated in Figure 3. It leverages features from two different sources to represent attention. In ITFM, to capture channel-wise attention, we employ adaptive pooling and  $1 \times 1$  convolution to generate the query representation  $Q$  and key representation  $K$ . This design allows ITFM to effectively combine information from different sources and capture contextual dependencies.  $Q$  and  $K$  are derived by

$$Q, K = conv_{1 \times 1}(pool(concat(LN(x_{skip}), LN(x_{dec})))), \quad (1)$$

where the inputs from skip connection and up-sampling operator are  $x_{skip}$  and  $x_{dec}$ ,  $LN$  denotes layer normalization,  $concat$  signifies channel-wise concatenation,  $pool$  represents adaptive pooling operation, while  $conv_{1 \times 1}$  denotes the  $1 \times 1$  convolution. The attention map is formulated as

$$A = softmax((Q^T \otimes K) \cdot \alpha), \quad (2)$$

where  $\otimes$  denotes the matrix multiplication,  $T$  indicates the matrix transposing operation,  $\alpha$  is a trainable scaling param-

eter. Finally, we employ the two input features to represent value V. The fused features can be expressed as

$$x = conv_{1 \times 1}(A \otimes (conv_{1 \times 1}(concat(x_{skip}, x_{dec})))^T) \quad (3)$$

Our representations Q and K are tailored to encompass singular global spatial features, leading to a substantial reduction in computational overhead.

## 2.2. Cross-level Multi-scale Interaction Module

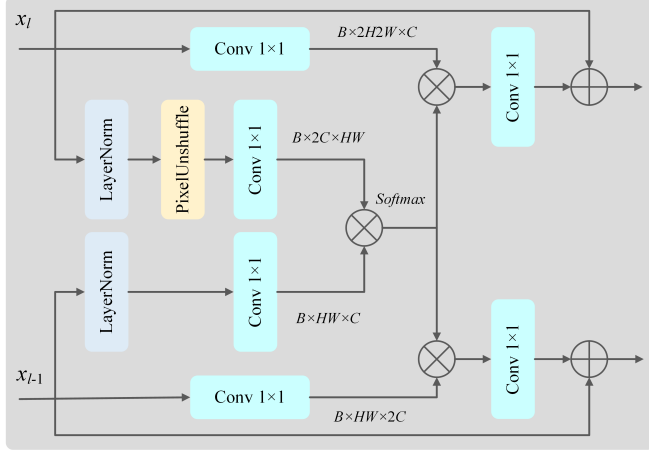


**Fig. 4.** Illustration of our proposed cross-level multi-scale interaction module (CMIM) that facilitates features interaction from different levels.

To address the limitation that existing architectures [7, 18–20] lack the ability to establish effective interactions across different levels, we propose a novel cross-level multi-scale interaction module (CMIM) to facilitate global interaction. As depicted in Figure 4, we unify the features and bring them to the same resolution. Subsequently, we obtain the transposed self-attention by performing matrix transposition. The value representations obtained from the skip connection and up-sampling operation are preserved in sizes identical to their corresponding input features. In CMIM, Q and K are derived as

$$\begin{aligned} Q &= conv_{1 \times 1}(PU(LN(x_l))), \\ K &= conv_{1 \times 1}(LN(x_{l-1})), \end{aligned} \quad (4)$$

where  $PU$  denotes the pixel-unshuffle operation,  $x_l$  and  $x_{l-1}$  are the features from level  $l$  and level  $l-1$ . Moreover, the enhanced representations of  $x_l$  and  $x_{l-1}$  can be formulated as

$$\begin{aligned} x'_l &= x_l + conv_{1 \times 1}(A \otimes conv_{1 \times 1}(x_l)), \\ x'_{l-1} &= x_{l-1} + conv_{1 \times 1}(A^T \otimes conv_{1 \times 1}(x_{l-1})), \end{aligned} \quad (5)$$

where  $x'_l$  and  $x'_{l-1}$  denote the enhanced features. Our CMIM offers two key advantages. Firstly, it addresses the issue of information loss that commonly occurs due to the repeated up-sampling and down-sampling. Secondly, the multi-scale

features obtained from one level play a crucial role in enriching the features of the subsequent level.

## 2.3. Multi-view Progressive Extraction Block

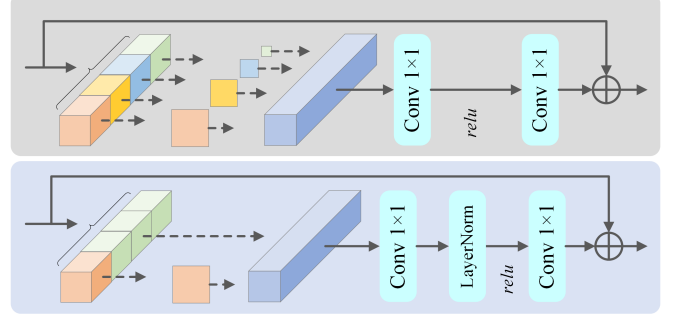


**Fig. 5.** Illustration of the basic learning block. *Top*: our proposed multi-view progressive extraction module. *Bottom*: the FasterNetBlock (FNB) with one fourth partial convolution.

Considering the high-resolution characteristics of remote sensing hazy images, we propose a novel multi-view progressive extraction block (MPEB). As illustrated in Figure 5, three-quarters of the features are divided into three parts, each corresponding to a grouped dilated convolution with different receptive fields. Although the sizes of the convolution kernels are not the same, they share the same dilation factors. This choice of constant dilation factors avoids the grid problem. The last one-quarter features are processed by only a  $1 \times 1$  convolution. The formulation of our MPEB is

$$\begin{aligned} x'_i &= conv_{2i-1 \times 2i-1, d, g}(x_i), i = 1, 2, 3, 4. \\ x &= mlp(concat(x'_1, x'_2, x'_3, x'_4)), \end{aligned} \quad (6)$$

where  $conv_{2i-1 \times 2i-1, d, g}$  denotes the convolution with kernel size of  $2i-1 \times 2i-1$ , dilation factor of  $d$  and group size of  $g$ .  $d$  and  $g$  conform to the follow

$$d = \begin{cases} 1, & i = 1 \\ 3, & otherwise \end{cases}, g = \begin{cases} 1, & i = 1 \\ \frac{1}{4}c, & otherwise \end{cases}, \quad (7)$$

where  $c$  denotes the channel number of input features.

## 3. EXPERIMENTS

### 3.1. Implementation Specifications

RSHazeNet is trained for a total of 1,000 epochs using a single NVIDIA GeForce RTX 3090 GPU with patch size and batch size of  $512 \times 512$  and 14, respectively. We utilize the Adam optimizer with an initial learning rate of 0.0002, which is gradually decreased to  $1 \times 10^{-8}$  using cosine annealing decay. During training, we apply data augmentation techniques such as random rotation and horizontal flipping.

**Table 1.** Remote sensing image dehazing results on StateHaze1K and RS-Haze datasets [7, 21]. Our proposed RSHazeNet obtains the best performance on all these testing remote sensing hazy datasets.

Method	StateHaze1K-thin			StateHaze1K-moderate			StateHaze1K-thick			StateHaze1K-average			RS-Haze		
	PSNR	SSIM	MSE	PSNR	SSIM	MSE	PSNR	SSIM	MSE	PSNR	SSIM	MSE	PSNR	SSIM	MSE
DCP [22]	13.15	0.7246	0.0473	9.780	0.5735	0.1072	10.25	0.5850	0.0942	11.06	0.6477	0.0832	17.86	0.7340	0.0201
AOD-Net [4]	19.54	0.8543	0.0113	20.10	0.8854	0.0101	15.92	0.7313	0.0265	18.52	0.8234	0.0159	27.09	0.8476	0.0032
GridDehazeNet [23]	24.34	0.9155	0.0037	23.05	0.9274	0.0051	20.24	0.8312	0.0096	22.54	0.8916	0.0061	35.23	0.9446	0.0004
FCFT-Net [13]	23.59	0.9127	0.0044	22.88	0.9272	0.0055	20.03	0.8156	0.0101	22.17	0.8852	0.0067	33.28	0.9417	0.0007
H2RL-Net [15]	20.91	0.8797	0.0083	22.34	0.9061	0.0065	17.41	0.7684	0.0228	20.22	0.8514	0.0125	31.18	0.9212	0.0019
4KDehazing [6]	22.35	<b>0.9550</b>	0.0059	23.73	0.9565	0.0047	20.61	<b>0.9264</b>	0.0088	22.23	0.9460	0.0065	33.80	0.9442	0.0007
M2SCN [9]	25.21	0.9175	0.0031	26.11	0.9416	0.0038	21.33	0.8289	0.0095	24.22	0.8960	0.0055	37.75	0.9497	0.0003
DehazeFormer [7]	<b>26.28</b>	0.9477	<b>0.0024</b>	<b>29.78</b>	<b>0.9677</b>	<b>0.0012</b>	<b>24.64</b>	0.9241	<b>0.0034</b>	<b>26.90</b>	<b>0.9465</b>	<b>0.0023</b>	<b>39.57</b>	<b>0.9701</b>	<b>0.0002</b>
<b>RSHazeNet</b>	<b>28.38</b>	<b>0.9666</b>	<b>0.0015</b>	<b>30.89</b>	<b>0.9717</b>	<b>0.0009</b>	<b>26.26</b>	<b>0.9325</b>	<b>0.0024</b>	<b>28.51</b>	<b>0.9569</b>	<b>0.0016</b>	<b>40.61</b>	<b>0.9754</b>	<b>0.0001</b>

### 3.1.1. Datasets

StateHaze1K dataset [21] comprises three subsets: StateHaze1K-thin, StateHaze1K-moderate and StateHaze1K-thick. Each subset consists of 400 image pairs, with 320 designated for training, 35 for validation, and 45 for testing purposes. RS-Haze dataset [7] is a large-scale dataset containing 51300 paired images for training and 2700 paired images for testing.

### 3.2. Comparisons to Existing Methods

Table 1 presents the evaluation results. Our RSHazeNet achieves the best performance in PSNR, SSIM, and MSE on both StateHaze1K and RS-Haze datasets. Specifically, our method outperforms DehazeFormer by an average of 1.61 dB on StateHaze1K dataset and 1.04 dB on RS-Haze dataset. Furthermore, we provide the visual comparisons, including DCP [22], AOD-Net [4], GridDehazeNet [23], DehazeFormer [7] and our RSHazeNet in Figure 6. It can be observed that our proposed method reconstructs haze-free images with the lowest error compared to the other methods.

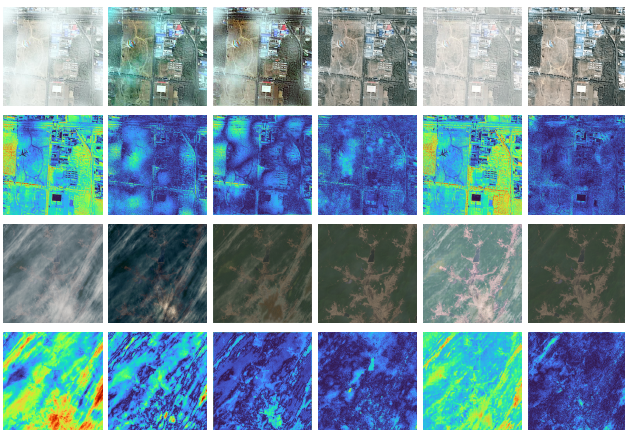


**Fig. 6.** Visual comparisons of input images, DCP [22], AOD-Net [4], GridDehazeNet [23], DehazeFormer [7] and our proposed RSHazeNet on Haze1K dataset [21] and RS-Haze dataset [7]. The subsequent row of each generated image is the corresponding error map.

### 3.3. Ablation Studies

The baseline architecture employ FNB [17] as the basic learning block and utilizes a  $1 \times 1$  convolution for intra-level feature fusion. We initially make modifications to the pipeline by adopting an encoder-minimal and decoder-minimal framework (EDF), which results in a slight improvement in performance while simultaneously reducing the computational burden. As illustrated in Table 2, our hierarchical framework surpasses the performance of the conventional u-shaped architecture by an improvement of 0.07 dB, while reducing the parameter count by 0.015% and the FLOPs by 11.83%. Subsequently, we undertake an exhaustive analysis of the contributions made by each module, encompassing IFTM, CMIM, MPEB, and soft residual connection (SRC) [7]. Each proposed component shows a positive effect on the overall performance.

**Table 2.** Ablation study of the individual components. Each proposed component plays a valuable role and shows a positive effect on the overall performance for remote sensing image dehazing.

Model	PSNR	SSIM	MSE	#Param	FLOPs
Baseline	21.95	0.8347	0.0094	1.105 M	38.89 G
+ EDF	22.02	0.8494	0.0093	1.088 M	34.29 G
+ IFTM	24.53	0.9186	0.0072	1.113 M	34.86 G
+ CMIM	25.24	0.9258	0.0033	1.213 M	40.42 G
+ MPEB	<b>26.12</b>	<b>0.9319</b>	<b>0.0026</b>	1.190 M	40.07 G
+ SRC	<b>26.26</b>	<b>0.9325</b>	<b>0.0024</b>	1.190 M	40.14 G

## 4. CONCLUSION

In this work, our proposed RSHazeNet represents a significant advancement in remote sensing image dehazing. By adopting an encoder-minimal and decoder-minimal architecture and introducing novel modules such as IFTM, CMIM, and MPEB, we have achieved a compelling trade-off between image quality and computational efficiency. Extensive experimental evaluations on multiple haze-degraded datasets demonstrate that RSHazeNet outperforms the state-of-the-art methods by a substantial margin.

## 5. REFERENCES

- [1] Tao Gao, Yuanbo Wen, Jing Zhang, Kaihao Zhang, and Ting Chen, “From heavy rain removal to detail restoration: A faster and better network,” *arXiv preprint arXiv:2205.03553*, 2022.
- [2] Xun Liu, Danfeng Hong, Jocelyn Chanussot, Baojun Zhao, and Pedram Ghamisi, “Modality translation in remote sensing time series,” *IEEE Transactions on Geoscience and Remote Sensing*, vol. 60, pp. 1–14, 2021.
- [3] Xiuchao Yue, Xiaoxuan Chen, Wanxu Zhang, Hang Ma, Lin Wang, Jiayang Zhang, Mengwei Wang, and Bo Jiang, “Super-resolution network for remote sensing images via preclassification and deep–shallow features fusion,” *Remote Sensing*, vol. 14, no. 4, pp. 925, 2022.
- [4] Boyi Li, Xiulian Peng, Zhangyang Wang, Jizheng Xu, and Dan Feng, “Aod-net: All-in-one dehazing network,” in *ICCV*, 2017, pp. 4770–4778.
- [5] Jeya Maria Jose Valanarasu, Rajeev Yasarla, and Vishal M Patel, “Transweather: Transformer-based restoration of images degraded by adverse weather conditions,” in *CVPR*, 2022, pp. 2353–2363.
- [6] Boxue Xiao, Zhuoran Zheng, Yunliang Zhuang, Chen Lyu, and Xiuyi Jia, “Single uhd image dehazing via interpretable pyramid network,” *Available at SSRN 4134196*, 2022.
- [7] Yuda Song, Zhuqing He, Hui Qian, and Xin Du, “Vision transformers for single image dehazing,” *IEEE Transactions on Image Processing*, vol. 32, pp. 1927–1941, 2023.
- [8] Trung Hoang, Haichuan Zhang, Amirsaeed Yazdani, and Vishal Monga, “Transer: Hybrid model and ensemble-based sequential learning for non-homogenous dehazing,” in *CVPR*, 2023, pp. 1670–1679.
- [9] Shuoshi Li, Yuan Zhou, and Wei Xiang, “M2scn: Multi-model self-correcting network for satellite remote sensing single-image dehazing,” *IEEE Geoscience and Remote Sensing Letters*, 2022.
- [10] Yuanjie Shao, Lerenhan Li, Wenqi Ren, Changxin Gao, and Nong Sang, “Domain adaptation for image dehazing,” in *CVPR*, 2020, pp. 2808–2817.
- [11] Zhengzhong Tu, Hossein Talebi, Han Zhang, Feng Yang, Peyman Milanfar, Alan Bovik, and Yinxiao Li, “Maxim: Multi-axis mlp for image processing,” in *CVPR*, 2022, pp. 5769–5780.
- [12] Ziqi Gu, Zongqian Zhan, Qiangqiang Yuan, and Li Yan, “Single remote sensing image dehazing using a prior-based dense attentive network,” *Remote Sensing*, vol. 11, no. 24, pp. 3008, 2019.
- [13] Yufeng Li and Xiang Chen, “A coarse-to-fine two-stage attentive network for haze removal of remote sensing images,” *IEEE Geoscience and Remote Sensing Letters*, vol. 18, no. 10, pp. 1751–1755, 2020.
- [14] Yufeng Huang and Xiang Chen, “Single remote sensing image dehazing using a dual-step cascaded residual dense network,” in *ICIP*. IEEE, 2021, pp. 3852–3856.
- [15] Xiang Chen, Yufeng Li, Longgang Dai, and Caihua Kong, “Hybrid high-resolution learning for single remote sensing satellite image dehazing,” *IEEE Geoscience and Remote Sensing Letters*, vol. 19, pp. 1–5, 2021.
- [16] Tao Gao, Yuanbo Wen, Kaihao Zhang, Peng Cheng, and Ting Chen, “Towards an effective and efficient transformer for rain-by-snow weather removal,” *arXiv preprint arXiv:2304.02860*, 2023.
- [17] Jierun Chen, Shiu-hong Kao, Hao He, Weipeng Zhuo, Song Wen, Chul-Ho Lee, and S-H Gary Chan, “Run, don’t walk: Chasing higher flops for faster neural networks,” in *CVPR*, 2023, pp. 12021–12031.
- [18] Shan Wang and Libao Zhang, “Dynamic mutual enhancement network for single remote sensing image dehazing,” in *ICIP*. IEEE, 2022, pp. 3336–3340.
- [19] Pengwei Dong and Bo Wang, “Transra: Transformer and residual attention fusion for single remote sensing image dehazing,” *Multidimensional Systems and Signal Processing*, vol. 33, no. 4, pp. 1119–1138, 2022.
- [20] Yuxia Bie, Siqi Yang, and Yufeng Huang, “Single remote sensing image dehazing using gaussian and physics-guided process,” *IEEE Geoscience and Remote Sensing Letters*, vol. 19, pp. 1–5, 2022.
- [21] Binghui Huang, Li Zhi, Chao Yang, Fuchun Sun, and Yixu Song, “Single satellite optical imagery dehazing using sar image prior based on conditional generative adversarial networks,” in *Proceedings of the IEEE/CVF winter conference on applications of computer vision*, 2020, pp. 1806–1813.
- [22] Kaiming He, Jian Sun, and Xiaoou Tang, “Single image haze removal using dark channel prior,” *IEEE transactions on pattern analysis and machine intelligence*, vol. 33, no. 12, pp. 2341–2353, 2010.
- [23] Xiaohong Liu, Yongrui Ma, Zhihao Shi, and Jun Chen, “Griddehazenet: Attention-based multi-scale network for image dehazing,” in *ICCV*, 2019, pp. 7314–7323.